

Origin and orbital distribution of the trans-Neptunian scattered disc

A. Morbidelli,^{1*} V. V. Emel’yanenko² and H. F. Levison³

¹*Observatoire de la Côte d’Azur, Boulevard de l’Observatoire, B.P. 4229, 06304 Nice Cedex 4, France*

²*South Ural University, Lenina 76, Chelyabinsk 454080, Russia*

³*Southwest Research Institute, 1050 Walnut St, Suite 426, Boulder, CO 80302, USA*

Accepted 2004 September 1. Received 2004 July 16; in original form 2003 September 29

ABSTRACT

We revisit the scenario proposed by Duncan and Levison in the late 1990s on the origin of the trans-Neptunian scattered disc. According to this scenario, the current scattered disc population is the remnant of a much more massive population that formed at the beginning of the Solar system, presumably when Neptune grew in mass. In order to compute the expected orbital distribution of the scattered disc bodies in the framework of this model, we have integrated the evolution of several thousands of test particles over the age of the Solar system, and looked at the orbital distribution of those surviving after more than 2×10^9 yr from their first scattering event. In order to compare this model distribution with the observed distribution, we have modelled the observational biases by generalizing a method originally introduced recently by Trujillo and Brown. Once the biases are taken into account, the model distribution matches the observed distribution fairly well. The most significant discrepancy is that the observed perihelion distance distribution is somewhat skewed towards larger perihelion distances than our model predicts. This is possibly due to the effects of planet migration (which tends to raise perihelion distances as recently shown by Gomes), which is not taken into account in our simulations.

Key words: celestial mechanics – Kuiper Belt – planets and satellites: formation – planets and satellites: individual: Neptune – Solar system formation.

1 INTRODUCTION

The existence of a trans-Neptunian scattered disc (SD) of objects was first predicted based on the study of the origin of Jupiter-family comets (Levison & Duncan 1997, hereinafter LD97, and references therein). LD97 found that the bodies that evolve from the Kuiper Belt to the Neptune-crossing region spend a considerable amount of time on Neptune – encountering orbits with a semi-major axes a larger than 30 au, before being transported either to the giant planets region ($a < 30$ au) or the Oort cloud ($a > 10\,000$ au). They therefore concluded that, associated with the Kuiper Belt, there should be a population of trans-Neptunian objects scattered by Neptune – which they named the *scattered disc*. In their view, the scattered disc was, relative to the Kuiper Belt, the analogue of the NEO population relative to the asteroid belt: a transient population, sustained in a sort of steady state by the reservoir population in the belt.

In a second paper, Duncan & Levison (1997, hereinafter DL97), gave another possible interpretation of the scattered disc. DL97 showed that, neglecting the flux of new objects from the Kuiper Belt, the SD population decays in number because of the leakage towards the giant planets region and the Oort cloud. However, this

decay is very slow: about 1 per cent of the population survives in the scattered disc for the age of the Solar system. Therefore, it is possible that the current SD population is the remnant of a (~ 100 times) more numerous population that formed at the beginning of the Solar system, presumably when Neptune grew in mass. Almost simultaneously, the first object with an orbit typical of the scattered disc (1996 TL₆₆) was discovered (Luu et al. 1997).

While in LD97’s view the number ratio between the Kuiper Belt and the SD populations was necessarily large (of order ~ 1000), in the view of DL97 there is a priori no causal relationship between the two numbers: the current SD population depends only on the original SD population, and not on the Kuiper Belt population.

The current discovery rate, once the relative observational biases are taken into account, suggests that the ratio between the SD and the Kuiper Belt populations is now close to 1/1 (Trujillo, Jewitt & Luu 2001). This fact rules out LD97’s model of the origin of the scattered disc, and seems to support that of DL97.

However, no one has ever checked whether the observed distribution of the SD population is even roughly consistent with that predicted by the DL97 model. Indeed, there are reasons to believe that the DL97 model does not include all the processes that may have been important during the formation of the SD. For example, Malhotra (1993, 1995), Gomes (2003) and Levison & Morbidelli (2003) showed that planetary migration most

*E-mail: morby@obs-nice.fr

probably occurred, and played an essential role in the sculpting of the Kuiper Belt. In addition, the discovery and orbital determination of 2000 CR₁₀₅ (Millis et al. 2000; Gladman et al. 2002) and of 2003 VB₁₂ (Brown et al. 2004) – with, respectively, $a \sim 230$ au, $q \sim 45$ au and $a \sim 530$ au, $q = 74$ au, q denoting the perihelion distance – revealed the existence of an *extended scattered disc population* that cannot be explained in the framework of the current planetary system as assumed by DL97 (Gladman et al. 2002; Morbidelli & Levison 2004). Moreover, Emel’yanenko, Asher & Bailey (2003) showed that five other objects, which are traditionally considered to be part of the SD population, never encounter Neptune during 4.5 Gyr simulations of their dynamical evolution. Therefore, there is now growing evidence that even DL97’s view is simplistic, and ‘something else’ has to have happened in the primordial Solar system.

Consequently, we think that it is timely and instructive to perform a quantitative comparison between the observed orbital distribution of the SD population and that expected in the framework of DL97’s scenario, which is precisely the goal of this work. In Section 2 we describe how we set up our numerical simulations for the construction of a model of the SD orbital-magnitude distribution, in the framework of DL97’s scenario. Section 3 discusses the observational biases and explains how a model distribution can be effectively compared with the observed distribution. Section 4 shows the results of such a comparison. Conclusions and discussions are reported in Section 5.

2 CONSTRUCTION OF A SCATTERED DISC DISTRIBUTION MODEL

In order to build a model of the distribution of SD bodies corresponding to the DL97 scenario we could in principle have used the original DL97 simulations. We have decided not to do so, and to use a new set of numerical simulations for, mainly, three reasons: (i) DL97 had a very limited number of particles surviving in the scattered disc for a very long time, (ii) the initial conditions in DL97 had very small inclinations, while it is now clear that the Kuiper Belt and the scattered disc are much more excited in inclination than they were thought to be in 1997, (iii) DL97 used an old version of the integrator (SWIFT_RMVS2; Levison & Duncan 1994) which might have behaved less accurately than the integrator later developed (SWIFT_RMVS3).

We have integrated 6414 test particles, initially uniformly distributed over $34.3 < a < 50$ au, $25 < q < 45$ au, $0^\circ < i < 60^\circ$, $0^\circ < (\omega, \Omega, M) < 360^\circ$. Different initial distributions can be tested a posteriori during the analysis of the results, by weighting each particle with an ‘existence function’ $P_0(a, q, i)$ that represents the probability that the particle exists in the new desired initial distributions. In practice we have tested only functions P_0 that are uniform in a and q , but have different dependences on i , as detailed in Section 4. The evolution of the particles has been computed using the SWIFT_RMVS3 integrator, over a total time-span of 4.5 Gyr, using a time-step of one year. The particles underwent the perturbations exerted by the sole four giant planets, which were initially placed on the current orbits. They were discarded from the integration when their perihelion distance decreased below 20 au or their semi-major axis exceeded 1000 au. Particles were considered ‘scattered’ if their semi-major axis changed with respect to the initial condition by more than 1.5 au, a value that, from the analysis of the orbital evolutions, appears considerably larger than the quasi-periodic oscillation of the semi-major axis of regular bodies in the trans-Neptunian region. For each scattered particle, we called ‘first scattering time’ (t_{1sc}) the first time that $|a(t) - a(0)| > 1.5$ au. This name is not totally appropri-

ate, because often the change in semi-major axis was due to a slow drift caused by a sequence of distant encounters with Neptune and not to one single event. Particles that never moved more than 1.5 au from the initial semi-major axis were considered stable Kuiper Belt members.

As recalled in the introduction, according to DL97 the current SD population is the remnant of a much larger population that has suffered scattering encounters with Neptune since the origin of the Solar system. In order to compute the expected orbital distribution of long-living scattered bodies, we should consider the orbital evolution of the integrated particles only starting at a time ΔT after their respective first scattering times (i.e. for $t > \Delta T + t_{1sc}$). The value of ΔT should be in principle close to the age of the Solar system. However, a value too close to 4.5 Gyr would severely limit the statistics on the orbital evolution of the surviving particles, because the window of time over which we would analyse our data (between $\Delta T + t_{1sc}$ and 4.5 Gyr) would be too narrow. A value of ΔT much smaller than 4.5 Gyr would conversely include the orbital evolution of particles which are still too ‘young’ from the dynamical point of view, thus producing an orbital distribution that presumably does not correspond to the one characterizing the current scattered disc population. After some attempts we have adopted the compromise solution $\Delta T = 2$ Gyr. With this choice, 38 particles contributed to the construction of the scattered disc orbital distribution model detailed below.

To construct the orbital distribution model, we have divided the (a, q, i) space in cells of width $1 \text{ au} \times 1 \text{ au} \times 2.5^\circ$, and we have computed the cumulative time spent in each cell by all the selected particles – each weighted by the existence function $P_0(a, q, i)$ – during the time $\Delta T + t_{1sc} < t < 4.5$ Gyr. The resulting ‘residence time distribution’ $R(a, q, i)$ can be regarded as the probability function that statistically describes the orbital distribution of the bodies that have spent at least 2 Gyr in the scattered disc and that had the imposed $P_0(a, e, i)$ distribution when they had their first scattering event. In the following we will restrict the function R to the region with $a > 50$ au for two reasons: (i) the initial conditions have $a < 50$ au, so that they are separated from the region under analysis, which makes the results less dependent on the exact choice of the initial conditions; and (ii) in the region with $a < 50$ au it is unclear which observed bodies are in the scattered disc and which have a stable resonant orbit, so that the comparison with observations would be delicate. As a matter of fact, this problem partially exists also beyond 50 au, particularly due to the existence of a group of objects in 2:5 resonance with Neptune (Chiang et al. 2003). We have numerically integrated over 1.2 Gyr the dynamical behaviour of the nine bodies in our scattered disc data base (see below) that have semi-major axes between 54 and 57 au. Only five seem to be associated with the 2:5 resonance, and all have chaotic orbits (one object has very irregular, large-amplitude librations, and four others show moderately irregular, moderate amplitude librations). Thus, in principle all might be scattered disc objects stuck in the resonance for very long times (DL97 found several of these cases). Consequently, we have decided to keep them in the scattered disc data base, against which our model distribution will be compared. In Section 5 we shall come back to our choice of selecting particles with $a > 50$ au and we shall discuss how the results would change if this selection criterion were dropped.

Concerning the absolute magnitude H , we assume a distribution $N(H) = 10^{\alpha H}$, with $4 \leq H \leq 15$ (no SD object has yet been discovered with an absolute magnitude outside this range), where α is a free parameter. The H -distribution is assumed to be independent of the orbital distribution.

In summary, our DL97-like scattered disc model is represented by four-dimensional normalized probability function $P(a, q, i, H) = R(a, e, i) \times N(H)$, and depends parametrically on the initial distribution $P_0(a, q, i)$ and on the exponent α of the absolute magnitude distribution.

3 OBSERVATIONAL BIASES

The orbital-magnitude distribution model developed in the previous section cannot be directly compared with the observations. In fact the observed distribution is severely affected by observational biases. We therefore need to model these biases and multiply the orbital magnitude distribution $P(a, q, i, H)$ by the bias function $B(a, q, i, H)$ to obtain a model biased distribution.

Unfortunately, the SD objects have been discovered by a variety of surveys, whose main characteristics (limiting magnitude, total sky area covered, pointing history, etc.) are often not publicly available. The problem has been circumvented by Trujillo & Brown (2001) in their work on the radial distribution of the Kuiper Belt beyond 50 au. The method that we have used is just a straightforward generalization of that used by Trujillo and Brown. Our implementation is detailed below.

We have taken from the Minor Planet Center the list of the SD objects with $a > 50$ au and $q > 25$ au, with multi-opposition orbits (43 objects, up to 2003 March 3). From the data reported at the MPC site (<http://cfa-www.harvard.edu/iau/lists/>), we have computed the apparent magnitude and ecliptic latitude of each object at the moment of its discovery, thus obtaining a list of couples $V_{\text{disc}}(k), L_{\text{disc}}(k)$, the index k running over the set of objects considered (1, ..., K). We assume that these quantities are not affected by measurement errors. The way to understand the following procedure is to consider each object as a pointer to a fictitious survey, which looked at magnitude V_{disc} and at latitude L_{disc} and found exactly one object. Consider one of these surveys, say the one corresponding to the k th object. For a set of parameters (a, q, i, H) , compute the probability $B_k(a, q, i, H)$ that an object with these parameters is discovered by the survey. This is the probability that the object has apparent magnitude V in the range

$$V_{\text{disc}} - \delta V < V < V_{\text{disc}} + \delta V$$

and latitude L in the range¹

$$L_{\text{disc}} - \delta L < L < L_{\text{disc}} + \delta L.$$

Therefore, $B_k(a, q, i, H)$ can be easily computed numerically, if one assumes that the values of the angles ω, Ω, M are random.² Repeat now the procedure for all sets of parameters (a, q, i, H) over the region covered by our orbital-magnitude distribution model, so that B_k becomes a tabulated function of (a, q, i, H) . The function B_k can be considered as the bias function for the survey k . Now multiply the model distribution $P(a, q, i, H)$ by the bias $B_k(a, q, i, H)$, thus obtaining a function $M_k(a, q, i, H)$ that describes the orbital-magnitude distribution of the objects that the k th survey could have discovered. Normalize M_k to unity, so that it becomes a probability distribution.

¹ We have used $\delta V = 0.1$ and $\delta L = 0.5$, but we have checked that this has no practical influence, provided that these values are small and are the same for all values of (a, q, i, H) and for all k .

² We have checked using numerical simulations that the angle ω of all the particles during the scattered phase has a fairly uniform distribution, which was not evident a priori.

Now repeat the procedure for all K fictitious surveys. Because each fictitious survey discovered the same number of objects (one each), the overall orbital-magnitude distribution of the objects discovered by all surveys is then simply

$$M(a, q, i, H) = \frac{1}{K} \sum_{k=1}^K M_k(a, q, i, H).$$

The function M describes our normalized model biased distribution of the SD objects.

In order to simplify the comparison with the observations, we introduce one-dimensional incremental distribution functions $m_a(a), m_q(q), m_i(i), m_H(H)$, computed by summing $M(a, q, i, H)$ over the hidden variables. Finally, these four functions are translated to cumulative distribution functions $m_a(a), m_q(q), m_i(i), m_H(H)$, which are compared with the cumulative distributions of the observed SD objects.

4 COMPARISON BETWEEN MODEL AND OBSERVATIONS

In this section we compare the cumulative semi-major axis, perihelion distance, inclination and absolute magnitude distributions of the observed SD objects with those predicted by our model biased distribution.

Among the SD population, we have considered all objects with $a > 50$ au and multi-opposition orbits, with the exception of those with $q < 25$ au (we stopped the simulations when $q = 20$ au, so that the model is artificially deficient of low- q objects) and of both 2000 CR₁₀₅ and 2003 VB₁₂ (which are evidently not part of the scattered disc in the sense of DL97; Gladman et al. 2002; Morbidelli & Levison 2004).

As detailed in Section 2, the model distribution depends on some free parameters. For the nominal results illustrated below, we have assumed that the exponent α of the H -distribution is 0.6, because this is well in the range of usually considered values 0.5–0.76 (see Trujillo & Brown 2001, for a review), but the dependence of the results on α will also be discussed. For the ‘existence function’ $P_0(a, q, i)$ (see Section 2) we have considered a uniform distribution in a and q within the ranges covered by our test particles. For the i distribution, we have adopted one characterizing the current ‘hot population’ of the Kuiper Belt, namely (Brown 2001)

$$P_0(i)di \propto \sin(i) \exp\left(\frac{-i^2}{2\sigma_i^2}\right) di, \quad (1)$$

with $\sigma_i = 12^\circ$. The rationale for this choice is that Gomes (2003) convincingly argued that the dynamically hot Kuiper Belt population was originally part of the scattered disc. How the results depend upon these parameters will be discussed below.

Fig. 1 compares the observed (dashed) and modelled (bold solid) semi-major axis distributions. To understand if the differences between the two distributions are significant or not we need to use a statistical test. The classical K–S test (Press et al. 1992) is not very suitable because it assumes that the model distribution is exact, and that the limited number of observational data (42 objects in our case) is the unique source of difference between the two distributions. In our case, the model has a large degree of uncertainty, given that it is constructed from the dynamical evolution of a very limited number of long-lived simulated particles (38 particles). Had we used a larger or smaller number of particles, the resulting model may have been significantly different. The standard K–S test does not account for this situation, but we can design a modified test, that

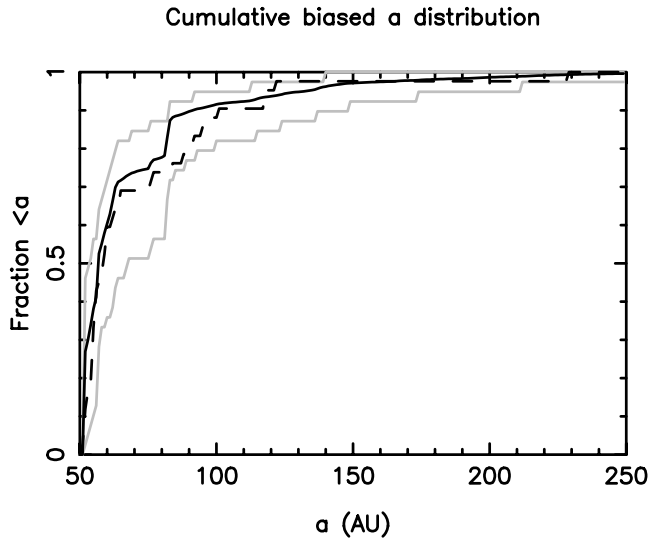


Figure 1. Dashed line: the cumulative semi-major axis distribution of the observed SD population (only objects with multi-opposition orbits, $a > 50$ au, $q > 25$ au and with the exception of 2000 CR₁₀₅ and 2003 VB₁₂ are considered). Solid black line: the cumulative semi-major axis distribution predicted by our model once the observational biases are taken into account. Solid grey curves: the boundaries of the 1σ uncertainty of our model, computed as explained in the text.

preserves the K–S philosophy, but is much more suitable in our case (see also appendix A in Levison, Morbidelli & Dones 2004). Let’s call the ‘reference model’ the one shown by the solid black curve in Fig. 1 and the ‘true observed distribution’ the one represented by the dashed curve. The difference Δ between the two distributions is quantified by the maximal absolute distance between the two curves. We then consider 100 new model distributions that we call ‘partial models’, constructed by taking into account only half of the particles, randomly selected among the 38 that constitute our reference model. From each of these partial models, we generate a ‘fake observed distribution’, by sampling the partial model distribution with 42 data points. We then measure the difference Δ_j ($j = 1, \dots, 100$) between the reference model and each of the fake observed distributions. The probability that the reference model is in statistical agreement with the true observed distribution is computed as the fraction of Δ_j values that are larger than Δ . We obtain 81 per cent. To give a graphical illustration, in Fig. 1 we have plotted two grey solid curves, defined such that, for each value of a , 68 per cent of the fake observed distributions fall within the curves, 16 per cent fall below the lower curve and the remaining 16 per cent fall above the upper curve. The grey curves therefore give a visual representation of the 1σ uncertainty region associated with our reference model. As one sees, the true observed distribution is within the 1σ uncertainty region for all values of a . Thus, our model is not in statistical disagreement with the observations. Notice also that there are no relevant discrepancies between model and observed distributions at ~ 55 au, where the 2:5 resonance with Neptune is located. This implies that the population of stable 2:5 resonant bodies, if any, is not (yet) prominent enough to pop out in our statistical analysis.

Of course, the 1σ uncertainty region would shrink if our reference model were computed from a much larger number of integrated particles. In this case, significant differences between model and observations would possibly become evident. However, it is not easy significantly to improve the orbital statistics on which the model is based. A brute force solution would be to increase the number of

particles in the initial conditions of our integrations. However, having already used 6414 particles, this situation cannot be significantly improved. Standard practice in a number of similar problems (see for instance Levison & Duncan 1997) is to ‘clone’ only the interesting particles, namely the 38 that participate in the construction of our reference model. However, this would not be an effective procedure in this case. The long-lived particles in the scattered disc are not very mobile in the orbital space; they typically stick to meta-stable regions, close to which they spend most of the time (for a discussion see LD97). If we clone stuck particles, there are two possible outcomes. If the clone is close enough to the original particle, it may stick to the same region. In this case, the clone behaves like the original particle and the effect in the overall residence time distribution $R(a, q, i)$ (see Section 2) is just amplified (which is precisely what we would like to avoid). Conversely, if the clone is far enough from the original particle to be free from the sticking effect of the parent meta-stable region, it will most probably be rapidly scattered by Neptune and eliminated in a short time. In this case, its contribution to the residence time distribution would be marginal.

We now move on to consider the perihelion distance distribution. In Fig. 2 the model (solid) and observed (dashed) distributions match almost perfectly up to $q = 36$ au. Beyond this value, the two distributions diverge, the observed one having significantly more bodies with large perihelion distance than the modelled one. The observed distribution goes well outside of the 1σ uncertainty region (dark grey solid curves) associated with our model distribution. Despite this, our modified K–S test gives a probability of 72 per cent that the model and the observed distribution are statistically equivalent (this is due to the large variability in the model distributions at the low- q end). Moreover, the 2σ uncertainty region (light grey solid curves, which are computed so that 2 per cent of the fake observed distributions fall below the lowest curve or above the upper curve) overlaps with the observed distribution. Therefore, from a purely statistical point of view, we cannot rule out our model distribution.

We believe nevertheless that the difference between the observed distribution and our model distribution is significant from an astronomical point of view. In fact, it confirms the result due to Emel’yanenko et al. (2003) that five objects (2000 PH₃₀, 1995 TL₈, 26181, 1999 CC₁₅₈, 2000 YW₁₃₄, the first two already identified by

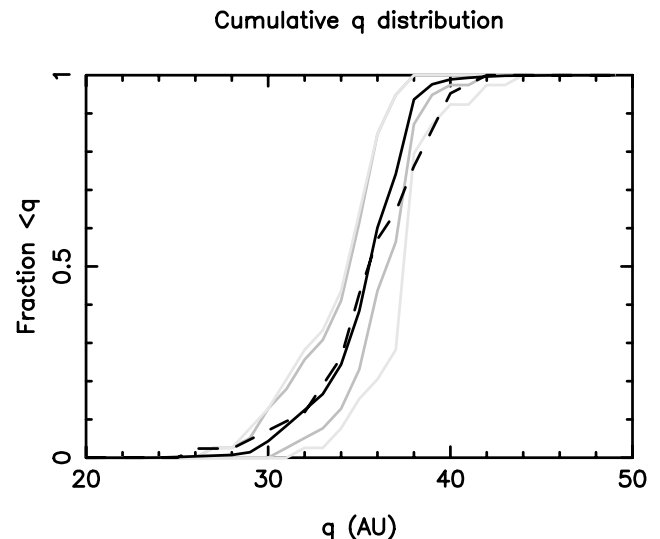


Figure 2. The same as Fig. 1, but for the perihelion distance distribution. The lightest grey curves show the boundaries of the 2σ uncertainty of our model.

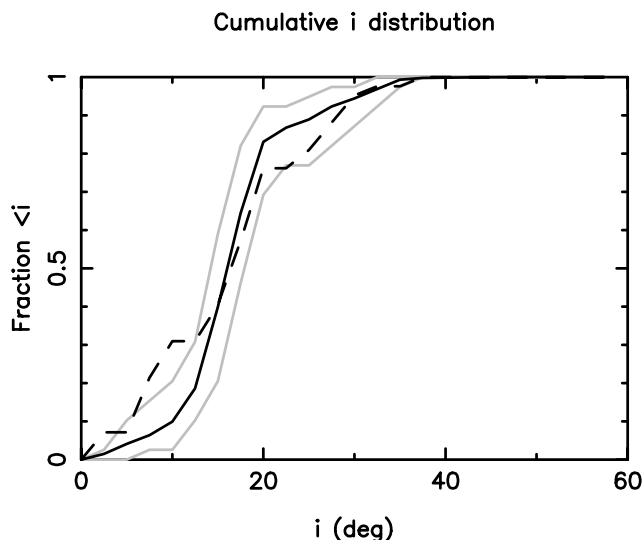


Figure 3. The same as Fig. 1, but for the inclination distribution.

Gladman et al. 2002) do not show significant change in their semi-major axes over 4 Gyr of numerical integrations. Emel’yanenko et al.’s result suggests that these objects are not scattered by Neptune and therefore cannot belong to a scattered disc structure produced by the giant planets on current orbits, as in the DL97 model. We have checked that if we eliminate these five objects from the observed population the match with our model perihelion distance distribution becomes excellent. Thus, we believe that the five objects belong to the *extended scattered disc* (ESD) population. They have probably been emplaced on to their current orbit during Neptune’s outward migration (Gomes 2003). We remind the reader that the most prominent ESD objects, 2000 CR₁₀₅ and 2003 VB₁₂ (q respectively of 45 and 74 au), have been excluded from our observed distribution from the very beginning, as it is clear that the origin of their peculiar orbits requires a strong perturbation from the ‘outside’ (such as a stellar encounter at ~ 1000 au; Morbidelli & Levison 2004).

Fig. 3 compares the observed and modelled inclination distributions. The model predicts with excellent accuracy the median value of the inclination of the discovered objects. Our modified K–S method gives a probability of 36 per cent that the model and the observed distributions are statistically equivalent. The value of σ_i (12°) used in equation (1) is what governs the median value of the model biased distribution. A larger value of σ_i shifts almost rigidly the model distribution towards the right, while a smaller value shifts it to the left.

Finally, Fig. 4 compares the observed and modelled absolute magnitude distributions. The agreement is excellent, except in the last bin. The reason for this discrepancy is not clear to us, but might be related to the inaccurate evaluation of the magnitude of the faintest discovered objects. Changing the exponent α in the assumed H -distribution within the typically accepted values (0.5–0.7) does not significantly change the model distribution. A lower value of α shifts the model distribution towards the left, improving the match with the observed distribution in the last bin, but making it worse on all other bins. A larger value of α shifts the model distribution towards the right, making worse the agreement with the observations.

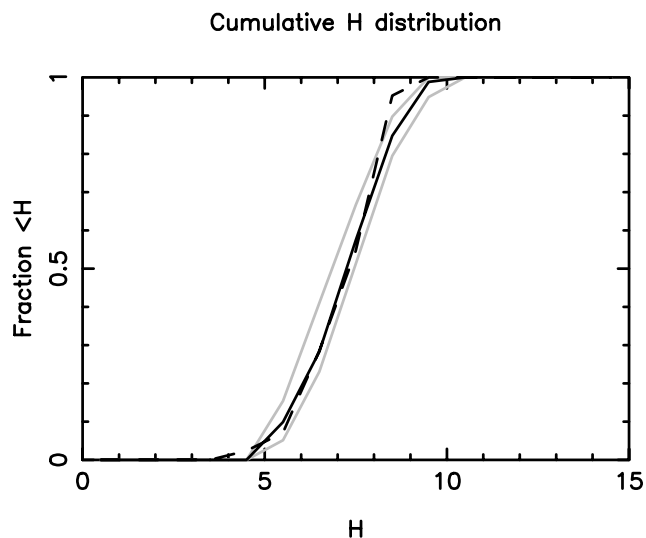


Figure 4. The same as Fig. 1, but for the absolute magnitude distribution.

5 CONCLUSIONS AND DISCUSSIONS

In this work we have developed a model of the orbital-absolute magnitude distribution of the SD population, according to the origin scenario designed in DL97. We remind the reader that, according to DL97, the current SD population is the remnant of a much more massive population (approximately $100\times$ more massive) that formed in the early Solar system. This population evolved under the effects of the perturbations exerted by the four current giant planets (no substantial planetary migration is assumed) and slowly decayed over the age of the Solar system.

An evaluation of the observational biases, done generalizing an original method introduced by Trujillo & Brown (2001), has allowed us to compare our model distribution with the observed distribution of SD objects. The statistical agreement between the two distributions is satisfactory. This is partially due to the fact that our model has an inherent large uncertainty, being based on the late evolution of 38. Had we been able to build a model based on a more solid statistics of the orbital evolutions of SD particles, it is possible that significant differences with the observed distribution would have become apparent.

On the basis of our result, we think that the DL97 scenario is basically correct for the origin of the scattered disc objects. We remind the reader that this scenario assumed the scattered disc was formed when the planets were in the current orbital configurations. We know that in reality the planets had to substantially migrate during the process of clearing of the planetesimal disc and formation of the scattered disc. The migration process is likely to increase the perihelion distance of some of the scattered objects, emplacing them into an extended scattered disc structure, mostly in the 50–100 au range (Gomes 2003). In fact, we see that the observed perihelion distance distribution of the objects beyond 50 au tends to have more bodies at large q than our model predicts, although the two distributions are in agreement at the 2σ level. And Emel’yanenko et al. (2003) found five bodies with $a < 100$ au that are not scattered by Neptune in 4-Gyr numerical integrations. The objects 2000 CR₁₀₅ and 2003 VB₁₂ are without ambiguity outside the perihelion distance distribution produced in the DL97 model (so that we excluded them from the observed distribution a priori), and the origin of their orbit is discussed in Morbidelli & Levison (2004).

Our study also provides the ground work for a more speculative consideration, concerning the original formation region of scattered disc objects. On this issue there are essentially two views. One is that these bodies formed in the giant planet region, namely in the semi-major axis range where orbits with zero eccentricity and inclination are unstable owing to the presence of the planets (approximately up to 35 au). Some of these bodies were transported outwards by close encounters with the planets, passed through the 35–50 au region, and reached the region beyond 50 au. In this view, the initial conditions that we have chosen for our integrations are intended to catch the distribution of the particles when they first transited through the 35–50 au region. The opposite view is motivated by the observation that the Kuiper Belt contains about 1 per cent of the primordial mass expected in the 40–50 au region (see Morbidelli, Brown & Levison 2003, for a review). It has been proposed that a strong excitation event moved most of the pristine Kuiper Belt objects to high eccentricity, where they started to encounter Neptune and to behave as scattered disc objects (Petit, Morbidelli & Valsecchi 1999). In this case, our initial conditions should represent the orbital distribution of the bodies soon after the excitation event.

Can our work help to discriminate between these two views? Maybe so. In the investigation reported above, we have considered the orbital distribution of the SD objects only beyond 50 au. If we do the same exercise extending the region of analysis to the domain with $a > 40$ au, our model predicts that 58 per cent of the observed SD objects should have $40 < a < 50$ au. As said above, it is not easy to distinguish the SD objects from the stable resonant objects in the region with $a < 50$ au. If we count as SD objects all the objects with $q < 35$ au in between the 2:3 and the 1:2 mean motion resonance with Neptune – which is certainly an overestimate – there are 17 SD objects with $40 < a < 50$ au as opposed to 42 objects with $a > 50$ au. Therefore, at most only 29 per cent of the observed objects have $a < 50$ au. The reason for this difference is, we think, that our initial conditions uniformly cover the (a, q) plane, and thus also sample regions where diffusion in the semi-major axis is very slow. Consequently, many particles (although moving by more than 1.5 au so as to be counted as ‘scattered’ in our analysis) never leave the 40–50 au region. These particles therefore dominate the residence time distribution. The deficit of observed SD objects with $a < 50$ au thus indicate that Nature, during the building process of the scattered disc, somehow avoided these slow-diffusing orbits. This suggests that the SD objects were originally inside 40 au, and were transported through the 40–50 au region following fast evolution tracks, dominated by strong encounters with Neptune. In this case, it is understandable that the objects preferentially avoided the regions where the dynamical evolution is the slowest. Conversely,

had the objects been placed in a Neptune-crossing orbit from the Kuiper Belt by some excitation event that increased their eccentricity, presumably the orbital space would have been sampled more evenly, and the slow diffusion regions could not have been avoided. This conclusion is in agreement with that of Gomes et al. (2003a), who showed that if most of the objects of an originally massive Kuiper Belt had been placed on Neptune-crossing orbits, Neptune would have migrated well beyond 30 au.

ACKNOWLEDGMENTS

This work has been supported by the INTAS grant 00-240, which has allowed VVE and AM to collaborate during mutual visits. We are also grateful for grant ACI 3142 CR3 from the French National Ministry of Research, which covered part of the expenses of HFL related to his sabbatical at Nice Observatory.

REFERENCES

- Brown M., 2001, *AJ*, 121, 2804
 Brown M. et al., 2004, *MPEC* 2004-E45
 Chiang E. I. et al., 2003, *AJ*, 126, 430
 Duncan M. J., Levison H. F., 1997, *Sci*, 276, 1670 (DL97)
 Emel’yanenko V. V., Asher D. J., Bailey M. E., 2003, *MNRAS*, 338, 443
 Gladman B., Holman M., Grav T., Kaavelars J. J., Nicholson P., Aksnes K., Petit J. M., 2002, *Icarus*, 157, 269
 Gomes R. S., 2003, *Icarus*, 161, 404
 Gomes R. S., Morbidelli A., Levison H. F., 2003, *Icarus*, 170, 492
 Levison H. F., Duncan M. J., 1994, *Icarus*, 108, 18
 Levison H. F., Duncan M. J., 1997, *Icarus*, 127, 13 (LD97)
 Levison H. F., Morbidelli A., 2003, *Nat*, 426, 419
 Levison H. F., Morbidelli A., Dones L., 2004, *AJ*, in press
 Luu J., Marsden B., Jewitt D., Trujillo C., Hergenrother C., Chen J., Offutt W., 1997, *Nat*, 387, 573
 Malhotra R., 1993, *Nat*, 365, 819
 Malhotra R., 1995, *Astron. J.*, 110, 420
 Millis R. L., Buie M. W., Wasserman L. H., Elliot J. L., Kern S. D., Wagner S. D., 2000, *BAAS*, 32, 1028
 Morbidelli A., Levison H. F., 2004, *AJ*, in press
 Morbidelli A., Brown M., Levison H., 2003, *Earth Moon and Planets*, 92, 1
 Petit J. M., Morbidelli A., Valsecchi G. B., 1999, *Icarus*, 141, 367
 Press W. H., Teukolsky S. A., Vetterling W. T., Flannery B. P., 1992, *Numerical Recipes in FORTRAN*, 2nd edn. Cambridge Univ. Press, Cambridge
 Trujillo C. A., Brown M. E., 2001, *ApJ*, 554, 95
 Trujillo C. A., Jewitt D. C., Luu J. X., 2001, *AJ*, 122, 457

This paper has been typeset from a $\text{\TeX}/\text{\LaTeX}$ file prepared by the author.